(2) According to the distribution of in-situ stress field in 4 # unit-blocks, the distribution law of initial in-situ stress field is very similar, but due to the different thickness of overlying surrounding rock, the values of stress components are different. As shown in Figure 10,the stress_x along the axis of the factory building is 4.33-13.95 MPa, the stress_y along the axis of the vertical factory building is 7.26-12.05 MPa, and the vertical stress_z is 5.88-10.75 MPa. The stress components in the factory building area increase with the decrease of elevation. The magnitude and direction of the stress components near the fault area have undergone obvious mutations, which are mainly confined to a certain distance near the fault area and tend to be stable far away from the fault area.

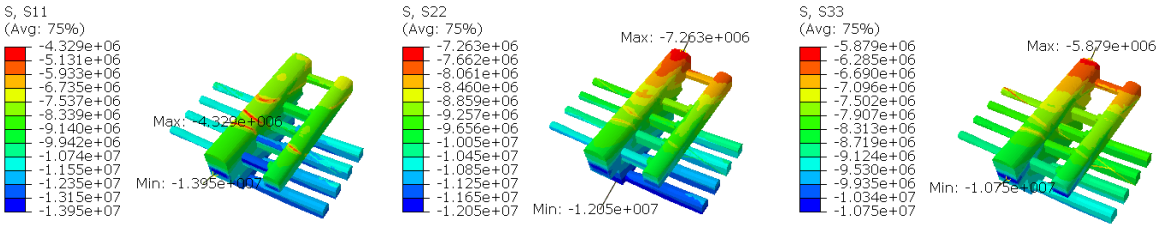

(a) Axis Direction (b) Downstream Direction (c) Vertical direction

Fig.10 Diagram of principal stress component distribution in caverns (Unit: Pa)

(3)As illustrated in Figure 11,the maximum principal stress of the main powerhouse is between 8.48 and 15.72 MPa, and the maximum compressive stress is at the bottom of the catchment well near the 1 # unit section of the main powerhouse; the minimum principal stress is between 1.22 and 10.01 MPa, and the minimum principal stress is at the junction of the main transporting tunnel and the fault F6. The rock mass in this area mainly consists of amphibolite schist, chlorite amphibolite schist, mica quartz schist, marble strip and altered chlorite amphibolite schist. The uniaxial saturated compressive strength is 40-60 MPa, which belongs to harder rock. The maximum principal stress of the main transformer chamber is between 9.31 and 14.37 MPa, the maximum compressive stress is at the bottom of the end wall of the main transformer chamber of pile No. CZ0+127.300, the minimum principal stress is between 1.24 and 9.74 MPa, and the minimum principal stress is near the arch where the main transformer tunnel intersects the fault F6.

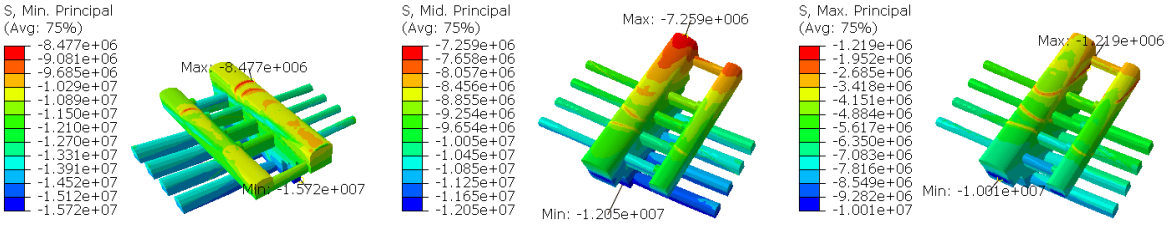

(a) maximum principal stress (b) Intermediate Principal Stress (c) Minimum principal stress

Fig.11 Schematic diagram of principal stress distribution in caverns model(Unit: Pa)

(4) The maximum principal stress and the minimum principal stress in the elevation plane in the generator layer is 11.05-14.49 MPa and 1.24-10.01 MPa respectively. The maximum principal stress in the elevation plane of bus layer is 10.75-14.49 MPa, and

the minimum principal stress is 3.06-8.35 MPa. The maximum principal stress in the elevation plane of the hydroturbine layer is 11.92-13.81 MPa, and the minimum principal stress is 3.72-7.78 MPa. It can be seen from the cross sections of hydroturbine layer, bus layer and generator layer in the workshop area that the initial in-situ stress at the same elevation varies due to the different thickness of the upper overburden layer. From the main workshop to the main transformer room, the covering thickness decreases gradually, and the values of principal stress and normal stress (absolute value) also decreases gradually.

5.Conclusion

Taking a hydropower station in southwest China as an example, considering the topographic and geomorphological characteristics of the valley and the geological structure conditions, the in-situ stress of the underground caverns of the hydropower station is inverted by the finite element multivariate regression method. According to the calculation results, it can be found that the in-situ stress increases with the increase of burial depth. The three-dimensional stresses of σ_x, σ_y and σ_z are orthogonal to each other, and the relationship between the values is $\sigma_x > \sigma_y > \sigma_z$. The maximum principal stress of the main powerhouse is between 8.48 and 15.72 MPa, and the maximum compressive stress is located at the bottom of the catchment well near the 1 # unit section of the main powerhouse. The maximum principal stress of the main transformer chamber is between 9.31MPa and 14.37MPa, and the maximum compressive stress is located at the bottom of the end wall of the main transformer chamber of pile number CZ0+127.300. Therefore, in the excavation and construction of underground powerhouse, strict attention should be paid to the position of maximum compressive stress. At the same time, the axis layout of underground powerhouse should be parallel to the maximum principal stress direction of the initial in-situ stress field and perpendicular to the minimum principal stress direction, which is beneficial to the stability of surrounding rock after excavation. Through regression analysis of underground powerhouse area, the in-situ stress value of key points obtained is close to the measured stress value, which shows that the inversion effect is better. The inversion reflects the distribution law of in-situ stress in the underground powerhouse area, and provides a reasonable three-dimensional initial stress field for the stability analysis of the excavation process of the powerhouse area caverns.

REFERENCES

Chen, X. T. , & Li, L. . (2007). Inverse analysis of initial field stress for underground cavities of a hydropower project. Rock & Soil Mechanics, 2007, 28 (5): 1523-1530.

Fu,C.H., Wang,W.M., Chen,S.H. “Back analysis study on initial geostress field of dam site for Xiluodu hydropower project. Chinese Journal of Rock Mechanics and Engineering,25 (11): 2305-2312.

González de Vallejo, L.I., Hijazo,T.(2008), “A new method of estimating the ratio between in situ rock stresses and tectonics based on empirical and probabilistic analyses”. Engineering Geology, 101(3-4):185-194.

Grossberg, S.,(1988). “Nonlinear neural networks: principles,mechanisms, and architectures”. Neural Networks, 1(1):17-61.

Guo ,H.Z., Ma, Q.C., Xue,X.C.,(1983). “Analysis method of initial stress field of rock mass. Chinese Journal of Geotechnical Engineering, 5 (3): 64-75.

Guo,M.W,Li,C.,Wang,S.L,et al., (2008). Study on inverse analysis of 3-D initial geostress field with optimized displacement boundaries. Rock and Soil Mechanics, 2008, 29(5): 1269-1274.

Jian-Guo, Z. , Qiang-Yong, Z. , Wen-Dong, Y. , & Xin, Z. . (2009). Regression analysis of initial geostress field in dam zone of dagangshan hydropower station. Rock & Soil Mechanics, 30(10), 3071-3078.

Kartam, N., Flood, I., Garrett, J.H.,(1997). “Artificial Neural Networks for Civil Engineers: Fundamentals and Applications”. American Society of Civil Engineers, New York, USA.

Li, Y.S., Yin, J.M., Chen, J.P., et al., (2012). “ Analysis of 3D in-situ stress field and query system’s development basedon visual BP neural network”. Procedia Earth and Plan-etary Science, 5:64-69.

Mckinnon,S.(2001),“Analysis of stress measurements using a numerical model methodology”. International Journal of Rock Mechanics and Mining Sciences,38(5):699-709.

Ming, J. Z. , Ya, X. W. , & Fu, S. J. . (2002). Ann-based 3-d back analysis of initial stress in rock masses. Journal of Hohai University, 30(3):52-56.

Qiangyong, Z. , Wen, X. , Xiuyong, Y. , & Xiaoping, H. . (2015). Back analysis of initial geostress field for underground powerhouse zone of shuangjiangkou hydropower station. China Civil Engineering Journal. 2015, 48 (8): 86-95.

Saati, V., Mortazavi, A. (2011) ,“Numerical modelling of in situ stress calculation using borehole slotter test”. Tunnelling and Underground Space Technology, 26(1):172-178.

Xiangbo, Q. , Shucai, L. , Shuchen, L. . (2003). 3d geostress regression analysis method and its application. Chinese Journal of Rock Mechanics & Engineering, 22(10), 1613-1617.